Temperature Influence on GaN HEMT Equivalent Circuit

Giovanni Crupi, *Senior Member, IEEE*, Antonio Raffo, *Member, IEEE*, Gustavo Avolio, *Member, IEEE*, Dominique M. M.-P. Schreurs, *Fellow, IEEE*, Giorgio Vannini, *Member, IEEE*, and Alina Caddemi, *Member, IEEE*

***Abstract*—The purpose of this letter is to present an experimental analysis of the temperature effects on the small-signal equivalent circuit of a GaN HEMT. With the aim of contributing to the exploration and advancement of this technology for high-power and high-temperature applications, the major intrinsic RF figures of merit together with a recently reported effect (i.e., PDRZ) are deeply investigated versus ambient temperature.**

***Index Terms*—equivalent circuit, gallium nitride (GaN), high electron-mobility transistor (HEMT), temperature.**

I. Introduction

OVER the years, several studies have been conducted to analyze the impact of the temperature on the high-frequency performance of different types of transistors, such as silicon and gallium-arsenide FETs [1]-[4]. Recently, particular attention has been paid to investigate GaN HEMT performance versus temperature [5]-[12]. Although this type of FET is very well-suited for high-power and high-temperature applications at microwave and millimeter-wave frequencies, high operating temperature causes an enhancement of thermal phenomena and self-heating effect (SHE), limiting device performance and reliability. Within this context, the present letter is aimed at investigating the behavior of the small-signal equivalent circuit elements versus ambient temperature (T_a) for a GaN HEMT on SiC substrate, which is an excellent thermal conductor. This work extends our previous studies, in which the analysis has been limited to investigate DC and RF measurements without extracting the equivalent circuit model [8], [9]. Although extracting the equivalent circuit parameters is often time-consuming and challenging, their analysis is a crucial task for effectively contributing to the advancement of FET technology. This is because the equivalent circuit provides an essential feedback for device manufacturers and is a very powerful tool for circuit designers.

As recently demonstrated, the transistor extrinsic capacitances can lead to an increase of the real parts of the impedance (Z-) parameters at high frequencies [13]. This effect is referred to by the acronym PDRZ, standing for positive derivative of $Re(Z_{ij})$ versus frequency. GaN HEMTs with large gate width are prone to the PDRZ effect associated to the concurrence of the extrinsic capacitive and inductive contributions. This is because larger gate widths correspond to smaller impedances associated with both intrinsic capacitances and resistances, implying that the intrinsic terminals tend to be quicker shorted by increasing the frequency. In this letter, the PDRZ effect is analyzed versus T_a for the first time. Although the PDRZ shape depends on temperature through all the extrinsic element values, its disappearance can be achieved by subtracting appropriate values of the extrinsic capacitances. In line with the fact that the extrinsic capacitances are mostly temperature insensitive, the PDRZ effect is made to vanish at all studied temperatures by using the same values of extrinsic capacitances. Furthermore, the circuit elements and the major intrinsic RF figures of merit are investigated to identify and quantify the impact of T_a variations on device performance. In particular, to quantify the variation of the inertia of the intrinsic device in responding to signal changes, the temperature dependence of the intrinsic time constants is studied for the first time. Finally, it is worth pointing out that temperature rise degrades transistor performance under both small- and large-signal operations, because they are strongly correlated with each other [8].

II. Experimental Results

The studied device is an AlGaN/GaN HEMT on SiC substrate with a gate length of 0.7 μm and a gate width of 2x400 μm. The present analysis is based on scattering (S-) parameter measurements from 300 MHz up to 40 GHz at five case temperatures: 20°C, 35°C, 50°C, 65°C, and 80°C. Fig. 1 shows the small-signal equivalent circuit used to model the tested device. The equivalent circuit is composed by two sections: bias independent extrinsic (i.e., C_{pg}, C_{pd}, L_g, L_s, L_d, R_g, R_s, and R_d) and bias dependent intrinsic (i.e., C_{gs}, C_{gd}, C_{ds}, R_{gs}, R_{gd}, R_{ds}, g_m, and τ_m) elements.

The tested device exhibits the PDRZ effect. Therefore, the extrinsic capacitances are extracted with a commercial circuit simulator by increasing their values from zero until the PDRZ effect disappears from the de-embedded data, as proposed in [13]. The experimental results show that the PDRZ effect can be removed at all the analyzed temperatures by using the same

Manuscript received _____; accepted _____. This work was supported by FWO–Vlaanderen (Belgium).

G. Crupi and A. Caddemi are with the Department of Engineering, University of Messina, 98166 Messina, Italy (e-mail: crupig@unime.it).

A. Raffo and G. Vannini are with the Department of Engineering, University of Ferrara, 44122 Ferrara, Italy.

G. Avolio and D. M. M.-P. Schreurs are with the Electronic Engineering Department, KU Leuven, B-3001 Leuven, Belgium.

values of the extrinsic capacitances (C_{pg} = 47 fF and C_{pd} = 60 fF). This result is consistent with the fact that the extrinsic capacitances representing the capacitive coupling between the pads are mostly temperature insensitive [11, 12]. As an illustrative example, Figure 2 shows the behavior of $Re(Z_{22})$ before and after de-embedding the extrinsic capacitances at five different ambient temperatures. It is worth noting that $Re(Z_{ij})$ shifts towards higher values by increasing T_a, due to the larger extrinsic resistances. After de-embedding the extrinsic capacitances, the extrinsic resistances and inductances are respectively determined from the real and imaginary parts of the "cold" Z-parameters. Figure 3 reports the behavior of the extracted extrinsic inductances and resistances versus T_a. The extrinsic inductances representing the metal contact pads and access transmission lines exhibit only a very weak decrease with increasing T_a, consistently with the expectation of a minimal temperature sensitivity [3, 11, 12]. R_g exhibits a slight increase with T_a as it consists mainly of a metallization resistance. In agreement with the finding of a previous study based on TLM measurements [9], the increase of R_d and R_s with T_a can be attributed to higher values of the sheet resistivity of the semiconductor material rather than to the ohmic-contact resistivity. As the gate is placed closer to the source than to the drain for increasing the breakdown voltage, the sheet resistivity and then its temperature dependence have a stronger impact on R_d rather than on R_s. Although for sake of simplicity R_d and R_s are typically assumed to be bias independent, their thermal sensitivity implies also a dependence on the dissipated power (P_{diss}) [7].

After extracting the extrinsic elements, the intrinsic ones can be straightforwardly calculated from the intrinsic admittance (Y-) parameters at the bias point of interest by using conventional formulas and taking the average over the frequency range where they play a more dominant role. Figures 4(a)-4(d) illustrate the intrinsic elements of the equivalent circuit versus T_a at V_{GS} = -2 V and V_{DS} = 19.5 V. The significant reduction of both g_m and g_{ds} can be ascribed to the degradation of the electron transport properties at higher temperatures. The reported values of these two conductances are significantly higher than the intrinsic g_m and g_{ds} calculated from DC measurements (g_{mDC} and g_{dsDC}), due to the dispersion effects arising from traps and thermal phenomena (see Figure 4(e)). Both g_m and g_{mDC} decrease with increasing T_a, resulting in the positive consequence of diminishing the kink effect in S_{22} [9]. On the other hand, contrary to the case of g_{ds}, the values of g_{dsDC} are negative and its magnitude even decreases at higher temperatures. This is because the SHE leads to a negative g_{dsDC} but its impact is seen to be reduced by heating the device, due to the decrease of output current and, in turn, of P_{diss} at higher T_a. Depending on the device thermal resistance (R_{th}), the resulting decrease in P_{diss} reduces the channel temperature (i.e., $T_{ch}=T_a+R_{th}*P_{diss}$) [7]. Dispersion mechanisms affect both DC and RF performance but in a different way, since they modify the thermal and trap occupation states, which however remain ''frozen'' during device operation at frequencies above the dispersion cut-off frequency. Figure 4(f) reports the intrinsic unity current gain cut-off frequency (f_T) that is calculated as $g_m/(2\pi*(C_{gs}+C_{gd}))$. The achieved value of f_T is found to be degraded from 11.3 GHz to 9.1 GHz by increasing T_a from 20°C to 80°C. The observed reduction of f_T is mostly due to the reduction of g_m and even further enhanced by the increase of C_{gs}, while the observed reduction of C_{gd} has only a negligible role. On the other hand, the achieved reduction of g_{ds} allows achieving an increasing trend with temperature of the magnitude of the open-circuit voltage gain (A_V) that is given by g_m/g_{ds} (see Figure 4(g)). As a matter of fact, A_V results to be increased from 67.8 to 70.2 by increasing T_a from 20°C to 80°C. As expected, the intrinsic resistances R_{gs} and R_{gd} exhibit an opposite dependence on temperature to that of the intrinsic conductances g_m and g_{ds}. The observed increase of τ_m at higher T_a can be attributed to the reduction of the average electron velocity in the channel. Likewise, the other two intrinsic time constants τ_{gs} (i.e., $R_{gs}*C_{gs}$) and τ_{gd} (i.e., $R_{gd}*C_{gd}$) are found to be increased with increasing T_a (see Figure 4(d)). The time constants exhibit an almost linear increase with increasing T_a so that their temperature coefficients (TCs) can be estimated as $(\Delta\tau/\tau_0)/\Delta T_a$ with τ_0 evaluated at 20°C [6]: $TC(\tau_m)$=0.37%/°C, $TC(\tau_{gs})$=0.67%/°C, and $TC(\tau_{gd})$=1.03%/°C. As a result of the achieved increase of the three time constants modeling the intrinsic non-quasi-static effects, we can conclude that the inertia of the intrinsic transistor in responding to signal changes becomes higher by heating the device.

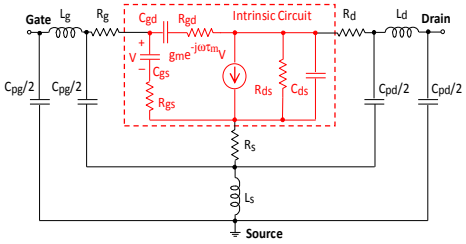

Fig. 1. Small-signal equivalent circuit for a HEMT.

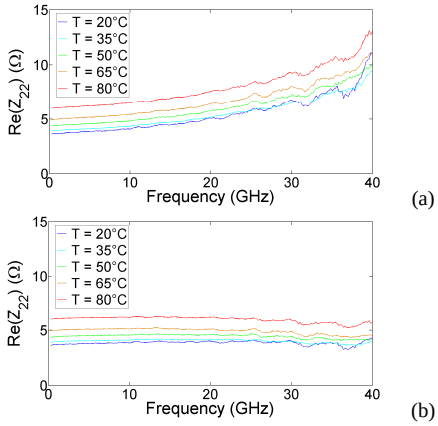

Fig. 2. Behavior of $Re(Z_{22})$, before (a) and after (b) removing the extrinsic capacitance contributions, as a function of frequency from 300 MHz to 40 GHz for a GaN HEMT at V_{GS} = 0 V and V_{DS} = 0 V under five different ambient temperatures.

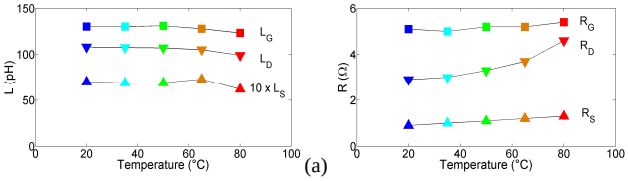

Fig. 3. Behavior of the extrinsic inductances (a) and resistances (b) versus ambient temperature for a GaN HEMT.

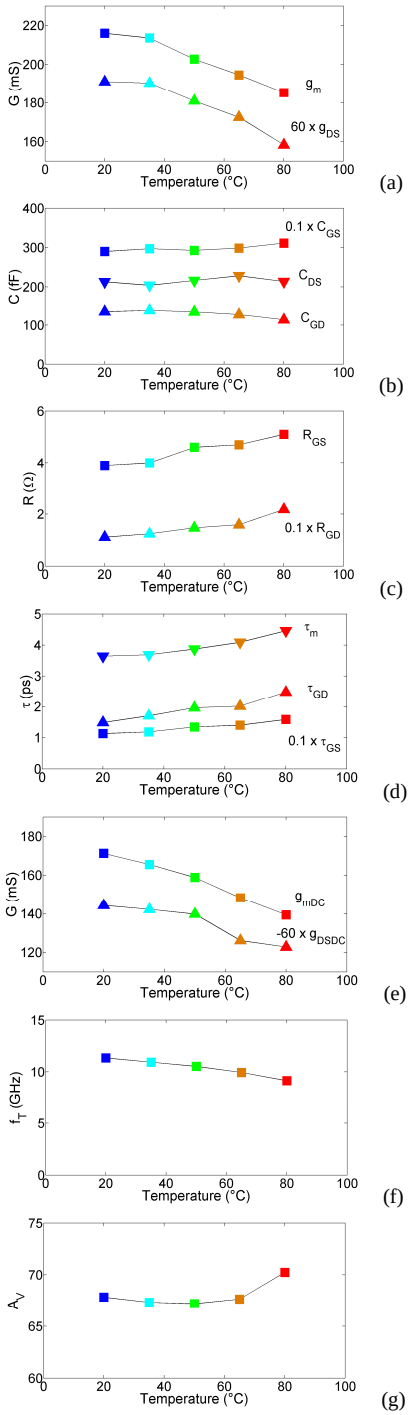

Fig. 4. Behavior of the intrinsic equivalent circuit elements and time constants (a)-(d), g_{mDC} and g_{dsDC} (e) the unity current gain cut-off frequency (f), and the open-circuit voltage gain magnitude (g) versus ambient temperature for a GaN HEMT at V_{GS} = -2 V and V_{DS} = 19.5 V.

III. Conclusions

We have extracted a small-signal GaN HEMT equivalent circuit as function of ambient temperature. We have focused on the PDRZ effect that cannot be traced back to any physical cause (e.g., traps and thermal phenomena) but is simply the frequency response due to extrinsic elements. This has been experimentally corroborated by showing that the PDRZ effect can be removed at all the studied temperatures by using the same values of the extrinsic capacitances, coherently with the fact that the extrinsic capacitances are substantially temperature insensitive. Moreover, the circuit elements and the major intrinsic RF figures of merit have been analyzed to determine how the device responds to ambient temperature increase. In particular, g_m and f_T have shown to be degraded, while A_V has found to be increased. For the first time, τ_m, τ_{gs}, and τ_{gd} have been studied to quantify the increase of the device inertia at higher temperatures. Finally, it has been shown how the temperature affects g_m and g_{ds} at both DC and RF.

References

[1] M. Emam, J. C. Tinoco, D. Vanhoenacker-Janvier, and J.-P. Raskin, "High-temperature RF behavior of partially-depleted SOI MOSFET transistors," *Solid State Electron.*, vol. 52, no. 12, pp. 1924-1932, Dec. 2008.

[2] J. C. Tinoco, B. Parvais, A. Mercha, S. Decoutere, and J.-P. Raskin. "DC and RF characteristics of FinFET over a wide temperature range," Proc. EuroSOI-2008. Cork, Ireland, Jan. 2008, pp. 57-58.

[3] A. R. Alt and C. R. Bolognesi, "(InP) HEMT small-signal equivalent-circuit extraction as a function of temperature," *IEEE Trans. Microw. Theory Techn.*, vol. 63, no. 9, pp. 2751-2755, Sep. 2015.

[4] M. A. Alim and A. A. Rezazadeh, "Temperature-dependent DC and small-signal analysis of AlGaAs/InGaAs pHEMT for high-frequency applications," *IEEE Trans. Electron Devices*, vol. 63, no. 3, pp. 1005-1012, Mar. 2016.

[5] O. Jardel, F. De Groote, T. Reveyrand, J.-C. Jacquet, C. Charbonniaud, J.-P. Teyssier, D. Floriot, and R. Quéré, "An electrothermal model for AlGaN/GaN power HEMTs including trapping effects to improve large-signal simulation results on high VSWR," *IEEE Trans. Microw. Theory Techn.*, vol. 55, no. 12, pp. 2660-2669, Dec. 2007.

[6] A. Darwish, B. Huebschman, E. Viveiros, and H. Hung, "Dependence of GaN HEMT millimeter-wave performance on temperature," *IEEE Trans. Microw. Theory Techn.*, vol. 57, no. 12, pp. 3205-3211, Dec. 2009.

[7] M. Thorsell, K. Andersson, M. Fagerlind, M. Südow, P.-Å. Nilsson, and N. Rorsman, "Thermal study of the high-frequency noise in GaN HEMTs," *IEEE Trans. Microw. Theory Techn.*, vol. 57, no. 1, pp. 3205-3211, Jan. 2009.

[8] G. Crupi, G. Avolio, A. Raffo, P. Barmuta, D.M.M.-P. Schreurs, A. Caddemi, and G. Vannini, "Investigation on the thermal behavior of microwave GaN HEMTs," *Solid-State Electron.*, vol. 64, no. 1, pp. 28-33, Oct. 2011.

[9] G. Crupi, A. Raffo, Z. Marinković, G. Avolio, A. Caddemi, V. Marković, G. Vannini, and D. M. M.-P. Schreurs, "An extensive experimental analysis of the kink effects in S22 and h21 for a GaN HEMT," *IEEE Trans. Microw. Theory Techn.*, vol. 62, no. 3, pp. 513-520, Mar. 2014.

[10] C. Wang, Y. Xu, X. Yu, C. Ren, Z. Wang, H. Lu, T. Chen, B. Zhang, and R. Xu, "An electrothermal model for empirical large-signal modeling of AlGaN/GaN HEMTs including self-heating and ambient temperature effects," *IEEE Trans. Microw. Theory Techn.*, vol. 62, no. 12, pp. 2878-2887, Dec. 2014.

[11] M. A. Alim, A. A. Rezazadeh, and C. Gaquiere, "Thermal characterization of DC and small-signal parameters of 150 nm and 250 nm gate-length AlGaN/GaN HEMTs grown on a SiC substrate," *Semicond. Sci. Technol.*, vol. 30, no. 12, pp. 1-10, Oct. 2015.

[12] M. A. Alim, A. A. Rezazadeh, and C. Gaquiere, "Small signal model parameters analysis of GaN and GaAs based HEMTs over temperature for microwave applications," *Solid-State Electron.*, vol. 119, pp. 11-18, May 2016.

[13] G. Crupi, D. M. M.-P. Schreurs, A. Caddemi, A. Raffo, F. Vanaverbeke, G. Avolio, G. Vannini, and W. De Raedt, "High-frequency extraction of the extrinsic capacitances for GaN HEMT technology," *IEEE Microw. Wireless Comp. Lett.*, vol. 21, no. 8, pp. 445-447, Aug. 2011.